Effects of substrate temperature on properties of Alq3 amorphous layers prepared by vacuum deposition

K. C. Chiu,* Z. A. Jian, Y. Z. Luo, J. M. Chung, S. J. Tang, M. C. Kuo and J. L. Shen
Department of Physics and Center for Membrane Technology,
Chung Yuan Christian University, Chung-Li, Taiwan 32023, ROC

W. C. Chou and C. S. Yang
Department of Electrophysics, National Chiao Tung University,
Hsin-Chu, Taiwan 300, ROC

ABSTRACT

In this report, various organic Alq3 amorphous layers are prepared by vacuum deposition at different substrate temperatures T_{sub} (from 30 to 180℃). The surface morphology, structural information, electrical and optical properties of these as-deposited layers are investigated by atomic force microscopy, X-ray diffraction, *J-E* curves, and photoluminescence studies, respectively. Furthermore, a temperature dependence of dark electrical conductivity $\sigma(T)$ deduced from *J-E* curves of these organic amorphous layers is presented. Finally, effects from T_{sub} on the physical properties of these organic Alq3 amorphous layers are discussed and a model based on a thermal interconversion between Alq3 isomers is proposed to explain these experimental results.

Keywords: Organic amorphous layer; Vacuum deposition; Electrical conductivity; Surface morphology; Photoluminescence; Isomeric transformation.

1. INTRODUCTION

Due to the processability advantages offered by organic materials, an intense research effort has been devoted to the preparation of organic thin-film field-effect transistors (OTFTs) during the last two decades [1-10]. The active layer in an OTFT is fabricated of small organic molecules [1-4], conjugated oligomers and polymers [5-10], or organic-inorganic hybrids. The performance of OTFTs involves the intramolecular and intermolecular charge transport mechanisms which are strongly affected by the structural and morphological characteristics of the as-deposited organic layer. Generally, organic layers from small molecules or conjugated oligomers [1-5] are prepared by vacuum deposition on cold substrate. These organic amorphous layers are not macroscopically homogeneous because of growth morphology defects [11]. In addition, during vacuum deposition in mass production, the latent heat released from vaporized molecule to its condensed phase may increase the real temperature of the unheated "cold" substrates (especially when a plastic substrate of poor thermal conductivity is used). From an external control and monitoring of the substrate temperature T_{sub}, our earlier experimental results indicated that, with slightly increasing T_{sub} (up to 60 ~ 90℃) to enhance the surface diffusion energy of the adhered molecules, the as-deposited Alq3 amorphous layers possess smaller surface roughness, larger electrical conductivity, and higher photoluminescence intensity [12]. For molecular C_{60} polycrystalline films, the effects from T_{sub} as well as the source temperature T_{sou} on the size, orientation, and crystallinity of the grains have been markedly observed [13,14]. In the case of oligothiophenes, the effects of T_{sub} on the structure and morphology of thin organic films have also been analyzed [5]. Thus, a systematic study on the effects from deposition conditions (extending to a wider range of T_{sub}) to the physical properties of the as-deposited organic layers should be very useful to the design, development, and fabrication of the future OTFTs.

In this report, as an example, various organic Alq3 layers are prepared by vacuum deposition at different T_{sub}. Alq3 is a stable metal chelate complex that can be sublimed to yield thin films with excellent electron-transport and light-emitting properties; it stands as one of the most successful organic materials used in organic light-emitting diodes OLEDs and hence a great attention has been paid to this organic semiconductor [15-21]. In this work, effects

* E-mail: kcchiu@phys.cycu.edu.tw

Organic Field-Effect Transistors V, edited by Zhenan Bao, David J. Gundlach
Proc. of SPIE Vol. 6336, 63361A, (2006) · 0277-786X/06/$15 · doi: 10.1117/12.678161

of T_{sub} on surface morphology, structural information, electrical and optical properties of these as-deposited Alq3 amorphous layers are investigated by atomic force microscopy (AFM), X-ray diffraction (XRD), current-voltage (*I-V*) curves, and photoluminescence (PL) studies, respectively. Furthermore, a temperature dependence of dark electrical conductivity $\sigma(T)$ deduced from *I-V* curves of these organic amorphous layers is presented. Finally, a model based on a thermal interconversion between Alq3 isomers is proposed to explain these experimental results.

2. EXPERIMENTAL DETAILS

The Alq3 layers used in this work are prepared in a vacuum thermal evaporation chamber. The source powder is first loaded in a boron-nitride crucible. After the vacuum chamber reaches a base pressure of 3×10^{-5} Torr, the heating system then turns on. The source temperature T_{sou} is fixed at 250 ± 5℃. The ITO conducting glass plate is used as a substrate. The distance between source crucible and substrate is approximately 16 cm. The values of T_{sub} are varied from 30℃ to 180℃ (note that the glass-transition temperature $T_g \cong 175$℃ for Alq3). When T_{sou} and T_{sub} attain the setting values, the shutter in between source crucible and substrate is then removed to allow vacuum deposition. The typical deposition time is 25 min. The thickness of the as-deposited layers is around 4000 Å. The thickness of the layer is first monitored by a quartz crystal deposition controller *in situ*, and then it is also corrected by a spectral reflectance method after the sample being removed out of the deposition chamber.

For electrical characterization, a top Au-metal contact with active area of about 4×4 mm^2 and thickness of about 1000 Å is fabricated by ion-sputtering. To reduce the thermally driven diffusion of Au atoms into the sample, the experimental parameters of ion-sputtering are controlled such that the temperature of the sample immediately after sputtering is within a reasonable range. For *I-V* measurements, an electrometer (in a current-voltage mode) is applied to the sandwiched Au/organic-layer/ITO samples. Due to the small resistance for some of the sandwiched organic samples, the small series resistance from the measurement circuit (especially for the sheet resistance from ITO film) has to be taken into account. Then, current density versus electric field (*J-E*) curves for various organic samples are deduced from *I-V* curves. With low fields being applied (from 0 to 0.75 MV/m), the *J-E* curves measured from all the samples exhibit a linear ohmic behavior [11], and hence, the dark electric conductivity σ of the organic Alq3 layer is then estimated. To eliminate effects from water vapor and oxygen gas, the measurements are conducted after the sample being put into a cryostat system under dynamic vacuum for at least 2 h. The data are taken and averaged during the next 10 h to check their stability and reliability at 300 K. The experimental results indicate that after 12 h in dynamic vacuum condition the electrical conductivities $\sigma(T = 300\text{K})$ for our amorphous layers are found to reach nearly steady state. Then, a temperature dependence (T varies from 300 ~ 40K) of the dark electrical conductivity $\sigma(T)$ of the amorphous layers is performed.

3. RESULTS AND DISCUSSION

Figure 1 shows the typical AFM pictures for the as-deposited Alq3 layers with respect to different T_{sub}. The calculated values of root-mean-square roughness (R_{rms}) are shown in Fig. 2. With slightly increasing T_{sub} from 30℃ up to 60℃, the as-deposited layers are found to possess flatter surface morphology with smaller R_{rms}. However, for $T_{sub} \fallingdotseq 90$℃, the surface roughness of the amorphous layer reaches a local maximum [12]. Further increase of thermal energy with $T_{sub} \fallingdotseq 120$℃, the surface roughness of the amorphous layer again possess flatter surface and R_{rms} reaches a local minimum. Finally, with increasing T_{sub} from 120℃ up to 180℃, R_{rms} increases. Also from the XRD patterns, an amorphous character with a broad diffuse peak representing an average nearest-neighbor bond length [11] is shown in Fig. 3 for all of the as-deposited films.

Figure 4 gives the room temperature normalized PL spectra for various Alq3 amorphous layers deposited at different T_{sub}. The incident pumping light is a beam of wavelength 396 nm from a semiconductor-laser. The luminance intensity from sample deposited at $T_{sub} = 60$℃ is much higher (which can be detected directly by the eyes during the experiments) than that from other samples. By comparing Figs. 2 and 4, one can find that the PL intensity peak of the sample is approximately inverse proportional to the roughness of the sample. This finding reveals that the surface morphology of the amorphous layer plays an important role in the luminance efficiency of OLEDs. Then, to investigate the PL intensity peak shift with respect to T_{sub}, from a Gaussian fit for each curve (but only the points

above 90% of its maximum intensity are taken for fitting due to the asymmetric character), the PL intensity peaks are 532.8 nm (for T_{sub} = 30℃), 532.0 nm (60℃), 526.4 nm (90℃), 529.0 nm (120℃), 531.2 nm (150℃), and 529.7 nm (180℃), respectively. The average PL intensity peak is about 530 ± 3 nm with half-amplitude bandwidth of 120 nm, which is consistent with the published results [12,16]. In addition, the PL intensity peak is observed to have a small blue-shift for T_{sub} varying from 30℃ to 90℃.

Under dynamic vacuum condition for at least 12 h, $\sigma(T = 300K)$ for various samples deposited at different T_{sub} are shown in Fig. 5. From this figure, one can see that the value of σ(300K) of the as-deposited Alq3 amorphous layers increases with increasing T_{sub} for T_{sub} = 30 ~ 90℃, drops down to a local minimum at $T_{sub} \fallingdotseq$ 120℃, and then increases with increasing T_{sub} again for T_{sub} = 120 ~ 180℃.

To test the thermal stability of physical properties for various amorphous Alq3 layers deposited at different T_{sub}, we perform a temperature dependence of dark electrical conductivity, $\sigma(T)$. As shown in Fig. 6 with back-and-forth temperature scan (T-scan) and with a cooling/heating rate of about 2 K/min, several interesting features are observed. (1) For amorphous Alq3 layers deposited at T_{sub} = 30℃, the values of σ slightly jump back and forth with decreasing T. But once reaching to the lowest T of 40K and then with increasing T, for T > 110K σ starts to deviate from its corresponding value measured at previous T-scan. For T = 300K, the ratio of the second measured value of σ to the first one after a complete T-scan, *i.e.*, $\sigma(T = 300K, 2^{nd})/\sigma(T = 300K, 1^{st})$, is about 0.73. (2) For amorphous layers deposited at T_{sub} = 60℃, 90℃, and 180℃, the variation of σ versus T is rather small, and these layers exhibit high thermal stability. The ratios of $\sigma(T = 300K, 2^{nd})/\sigma(T = 300K, 1^{st})$ for layers deposited at T_{sub} = 60℃, 90℃, and 180℃ are 0.90, 0.94, and 0.96, respectively. (3) For amorphous layers deposited at T_{sub} = 120℃ and 150℃, an abrupt decrease during the first decreasing T-scan is observed. Once dropped into the lowest-σ state, σ becomes less sensitively dependent on T. The ratios of $\sigma(T = 300K, 2^{nd})/\sigma(T = 300K, 1^{st})$ for amorphous layers deposited at T_{sub} = 120℃ and 150℃ reduce exaggeratedly down to 0.67 and 0.31, respectively. These findings strongly reveal that σ of the amorphous layers deposited at T_{sub} = 120℃ and 150℃ is under irreversible change with respect to the first cooling-down process.

Above experimental results from Figs. 1-6 clearly show that the physical properties of the as-deposited Alq3 amorphous layers are strongly affected by T_{sub}, especially for an anomalous T_{sub}-dependence of physical properties as T_{sub} varies from 90℃ to 120℃. To explain these rich behaviors, at first, some important published results about Alq3 molecules and its condensed phases are summarized as in the following. There are two types of geometrical isomers for Alq3, namely, meridional (*mer*, C1 symmetry) and facial (*fac*, C3 symmetry); but the possibility of thermal interconversion between the *mer* and *fac* isomers when sublimed in high vacuum is still unclear [17]. Though such an isomeric transformation at around 115℃ was inferred from NMR measurements when dimethylsulfoxide was used as the solvent [17, 18]. From a detailed density functional theory study, the *mer* isomer is calculated to be lower in energy than the *fac* isomer by 0.17 eV [19]. For crystalline phases, α-Alq3 and β-Alq3 phases are identified as low temperature phases, while γ-Alq3 and δ-Alq3 phases are identified as high temperature phases (above 395℃) [17]. From ordered Alq3 films by molecular beam deposition on cleaved KCl and KBr substrates at room temperature, the growth of *mer* isomer crystals was suggested [20]. However, the high temperature δ-Alq3 phase being composed of *fac* isomers was identified [21].

Then, to explain the experimental results obtained by this work, we propose a model based on that a thermal interconversion between the *mer* and *fac* isomers occurs in between 90 ~ 120℃ when sublimed in high vacuum. For $T_{sub} \leqq$ 90℃, the vacuum deposition to form the amorphous layer is dominated by irregular stacking of *mer* Alq3 molecules. For $T_{sub} \geqq$ 120℃, the vacuum deposition from irregular stacking of *fac* Alq3 molecules may start to play a significant role.

For $T_{sub} \leqq$ 90℃, we assume that the vacuum deposition is dominated by irregular stacking of *mer* Alq3 molecules. With slightly increasing T_{sub} from 30℃ up to 60℃, the adhered Alq3 molecules gain more surface diffusion energy. This 2D surface-diffusion process leads the as-deposited Alq3 amorphous layers with flatter surface morphology and smaller R_{rms} as shown in Figs. 1-2. However, for $T_{sub} \fallingdotseq$ 90℃, this higher thermal energy may promote a preferential rearrangement of the short π-π contacts between the ligands of neighboring Alq3 molecules and results some prototypes of α-Alq3 or β-Alq3 crystallines [17,20]. Hence the surface roughness of the amorphous layer reaches a local maximum. For T_{sub} in between 30 ~ 90℃, the higher T_{sub} results the closer links between the ligands in *mer* Alq3 molecules. Therefore, for Alq3 layers deposited at higher T_{sub}, the easier charge-carrier-hopping leads to a higher value of $\sigma(T = 300K)$ as shown in Fig. 5; and, the stronger interaction between the ligands in *mer* Alq3 molecules results a small blue-shift of the PL intensity peak as abovementioned. In addition, from a study of $\sigma(T)$, this specific

3D stacking structure deposited at $T_{sub} \fallingdotseq 90℃$ (as comparing to those deposited at $T_{sub} \fallingdotseq 30℃$ and 60℃) can be rather robust upon cooling down to low temperatures as depicted in Fig. 6.

For $T_{sub} \geqq 120℃$, we suggest that the vacuum deposition from irregular stacking of *fac* Alq3 molecules may start to play a significant role. Since *fac* isomer has a higher dipole moment than *mer* isomer, and a stronger dipole-dipole interaction acts as a stabilizing factor in the aggregate phase [19]. As comparing to the amorphous layers deposited at $T_{sub} = 90℃$ which are dominated by *mer* Alq3 molecules, the amorphous layers deposited at $T_{sub} = 120℃$ possess a flatter surface with smaller R_{rms}. In addition, the *fac* isomer is reported to act as a trapping state in the electron transport [19]. Thus, the layers deposited at $T_{sub} = 120℃$ and 150℃ possess much smaller values of σ(300K) as shown in Fig. 5. Furthermore, the *fac* isomers in amorphous layers may not be stable below room temperatures. This is deduced from the theoretical calculation [19] and experimental facts [20,21]. Thus, during the first cooling down process, the *fac* isomers are not stable in their "as-deposited" amorphous states, and hence an abrupt discontinuity as observed in $\sigma(T)$ due to the conformation instability is resulted as shown in Fig. 6. For the second cooling down process (not shown in Fig. 6), the variation in $\sigma(T)$ measurement is much less. For $T_{sub} = 180℃$ above the glass transition temperature, the as-deposited Alq3 films may become more order. One would expect some crystalline characters to be observed in XRD pattern, but as shown in Fig. 3 an amorphous character is still presented. However, the experimental data from Figs. 1-2 indicate that some larger grains are formed. The values of σ for layers with larger grains (formed at high T_{sub} and hence with closer separation and stronger interaction between Alq3 molecules) reach maximum values again and are very stable against temperature changes as depicted in Figs. 5-6.

In contrast to inorganic covalent compounds, the effects of T_{sub} on the physical properties of these as-deposited organic amorphous layers from small molecules exhibit much complex and interesting behaviors. The intrinsic properties of isomeric transformation and complex interactions between ligands of these small organic molecules as well as the molecular dynamics from both bulk diffusion and interface diffusion can play significant roles for organic thin films fabricated by vacuum deposition. Thus, a detailed study on the effects from deposition conditions to the physical properties of these as-deposited organic layers should be very important to the design, development, and fabrication of the future OLEDs and OTFTs.

4. SUMMARY

In this report, various organic Alq3 amorphous layers are prepared by vacuum deposition at different T_{sub} from 30 ~ 180℃. Then, effects of T_{sub} on the surface morphology, structural information, electrical and optical properties of the as-deposited Alq3 amorphous layers are investigated. An anomalous T_{sub}-dependence of physical properties is observed for those Alq3 amorphous layers deposited at $T_{sub} \leqq 90℃$ and at $T_{sub} \geqq 120℃$, respectively. A model based on that, when Alq3 sublimed in high vacuum, a thermal interconversion between the *mer* and *fac* isomers occurs in between 90 ~ 120℃ is proposed to explain these anomalous experimental results. This research also indicates that the intrinsic properties of isomeric transformation and complex interactions between ligands of these small organic molecules as well as the molecular dynamics from both bulk diffusion and interface diffusion can play significant roles for organic thin films fabricated from small organic molecules by vacuum deposition.

ACKNOWLEDGEMENTS

The authors would like to thank the National Science Council (via NSC94-2112-M-033-002) and the Ministry of Education (via the Center-of-Excellence Program on Membrane Technology) of the Republic of China for financially supporting this research.

REFERENCES

[1] R. C. Haddon, A. S. Perel, R. C. Morris, T. T. M. Palstra, A. F. Hebard and R. M. Fleming, "C_{60} thin film transistors," *Appl. Phys. Lett*. 67(1), 121-123 (1995).

[2] Y. Y. Lin, D. J. Gundlach, S. F. Nelson and T. N. Jackson, "Pentacene-based organic thin-film transistors," *IEEE Trans. Elec. Dev.* 44(8), 1325-1331 (1997).
[3] H. E. Katz, A. J. Lovinger, J. Johnson, C. Kloc, T. Siegrist, W. LI, Y. Y. Lin and A. Dodabalapur, "A soluble and air-stable organic semiconductor with high electron mobility," *Nature* 404(6777), 478-481 (2000).
[4] D. J. Gundlach, J. A. Nichols, J. Zhou and T. N. Jackson, "Thin-film transistors based on well-ordered thermally evaporated naphthacene films," *Appl. Phys. Lett.* 80(16), 2925-2927 (2002).
[5] F. Garnier, "Thin-film transistors based on organic conjugated semiconductors," *Chem. Phys.* 227(1-2), 253-262 (1998).
[6] A. Tsumura, H. Koezuka, and T. Ando, "Macromolecular electronic device: field-effect transistor with a polythiophene thin film," *Appl. Phys. Lett*. 49(18), 1210-1212 (1986).
[7] J. H. Burroughes, C. A. Jones, and R. H. Friend, "New semiconductor device physics in polymer diodes and transistors," *Nature* 335(6186), 137-141 (1988).
[8] C. D. Dimitrakopoulos and P. R. L. Malenfant, "Organic thin film transistors for large area electronics," *Adv. Mater.* 14(2), 99-117 (2002).
[9] A. Pron and P. Rannou, "Processible conjugated polymers: from organic semiconductors to organic metals and superconductors," *Prog. Polym. Sci*. 27(1), 135-190 (2002).
[10] K. Bock, "Polymer electronics systems-polytronics," *Proc. IEEE* 93(8), 1400-1406 (2005).
[11] S. R. Elliott, *Physics of Amorphous Materials*, 2nd ed., Longman Sci. & Tech., Essex, 1990.
[12] J. M. Chung, Y. Z. Luo, Z. A. Jian, M. C. Kuo, C. S. Yang, W. C. Chou, and K. C. Chiu, "Effects of substrate temperature on the properties of Alq3 amorphous layers prepared by vacuum deposition," *Jpn. J. Appl. Phys.* 43(4A), 1631-1632 (2004).
[13] R. S. Chen, Y. J. Lin, Y. C. Su, and K. C. Chiu, "Surface morphology of C_{60} polycrystalline films from physical vapor deposition," *Thin Solid Films* 396(1-2), 103-108 (2001).
[14] W. R. Cheng, S. J. Tang, Y. C. Su, Y. J. Lin, and K. C. Chiu, "Effects of substrate temperature on the growth of C_{60} polycrystalline films by physical vapor deposition," *J. Cryst. Growth* 247(3-4), 401-407 (2003).
[15] Z. H. Kafafi, ed., *Organic Electroluminescence*, Taylor & Francis Group, London, 2005.
[16] D. S. Qin, D. C. Li, Y. Wang, J. D. Zhang, Z. Y. Xie, G. Wang, L. X. Wang, and D. H. Yan, "Effects of the morphologies and structures of light-emitting layers on the performance of organic electroluminescent devices," *Appl. Phys. Lett.* 78(4), 437-439 (2001).
[17] M. Brinkmann, G. Gadret, M. Muccini, C. Taliani, N. Masciocchi, and A. Sironi, "Correlation between molecular packing and optical properties in different crystalline polymorphs and amorphous thin films of *mer*-Alq3," *J. Am. Chem. Soc.* 122(21), 5147-5157 (2000).
[18] B. C. Baker and D. T. Sawyer, "Proton nuclear magnetic resonance studies of 8-quinolinol and several of its metal complexes," *Anal. Chem*. 40(13), 1945-1951 (1968).
[19] A. Curioni, M. Boero, and W. Andreoni, "Alq3: ab initio calculations of its structural and electronic properties in neutral and charged states," *Chem. Phys. Lett.* 294(4-5), 263-271 (1998).
[20] H. Ichikawa, T. Shimada, and A. Koma, "Ordered growth and crystal structure of Alq3 on alkali halide surfaces," *Jpn. J. Appl. Phy*. 40(3A), L225-L227 (2001).
[21] M. Colle, J. Gmeiner, W. Milius, H. Hillebrecht, and W. Brutting, "Preparation and characterization of blue-luminescent Alq3," *Ad. Funct. Mater.* 13(2), 108-112 (2003).

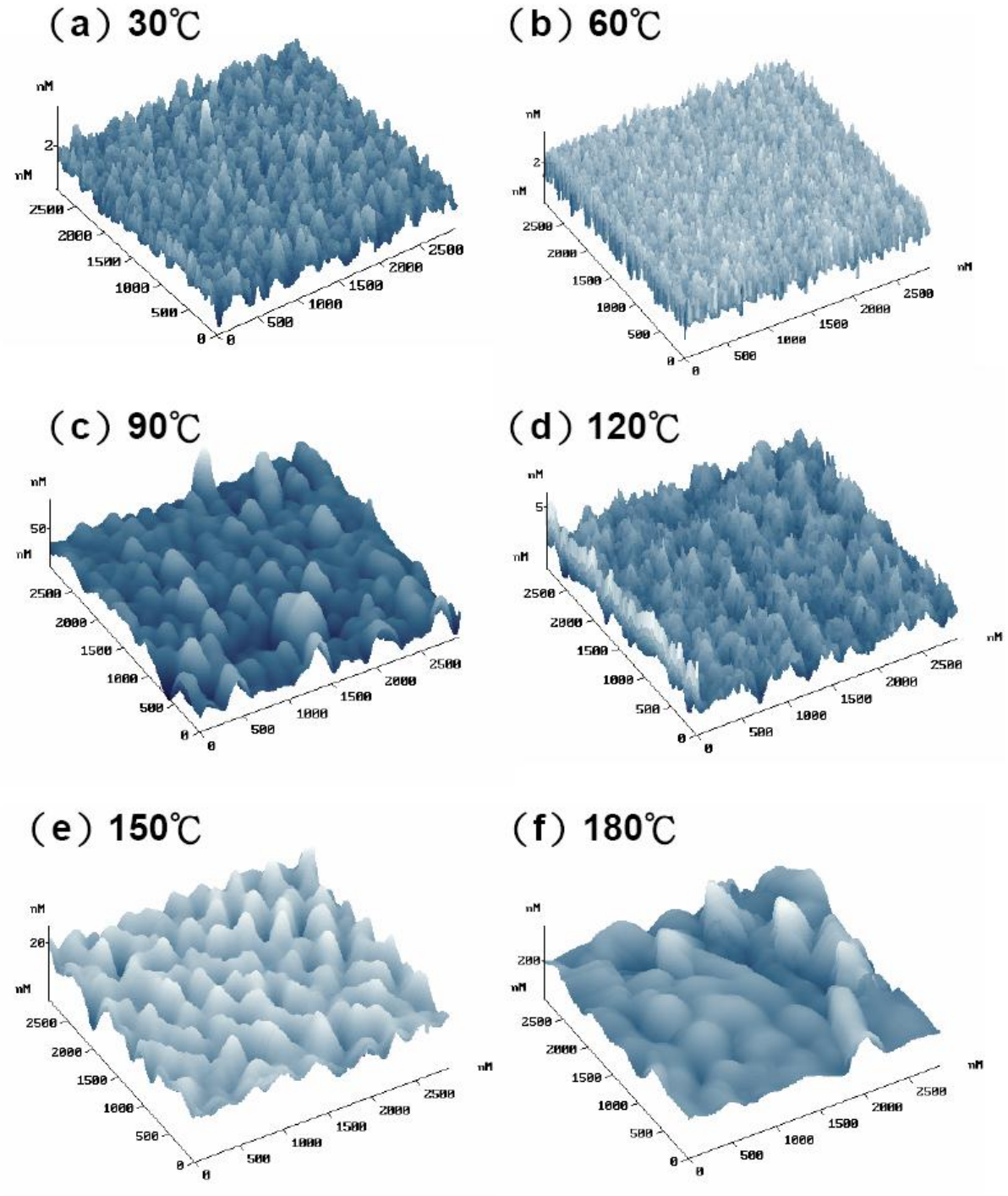

Fig. 1 AFM pictures for Alq3 layers with respect to different T_{sub}. Note the adjustment on vertical scales.

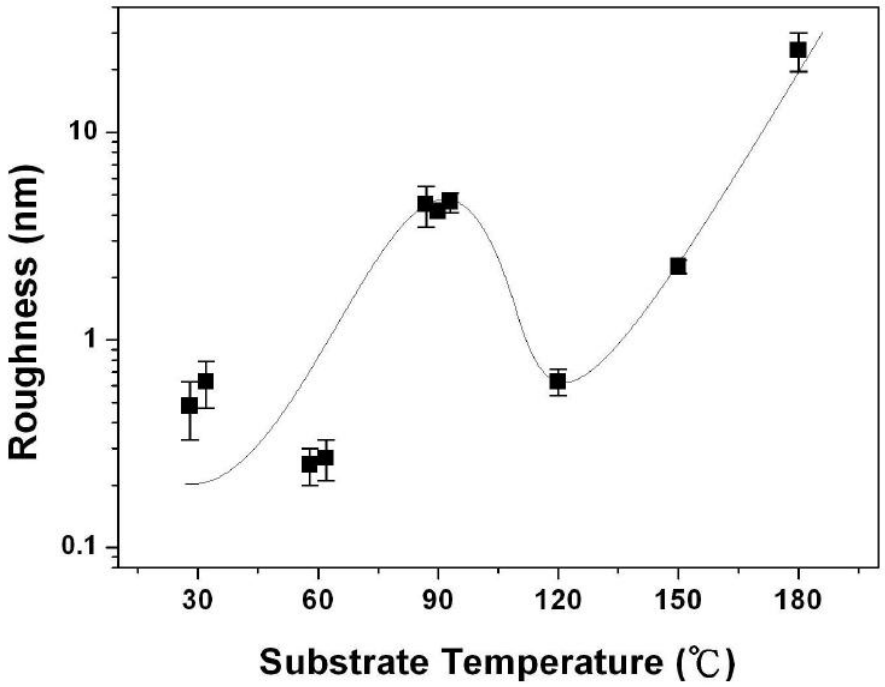

Fig. 2 Calculated values of R_{rms} for Alq3 layers with respect to different T_{sub}.

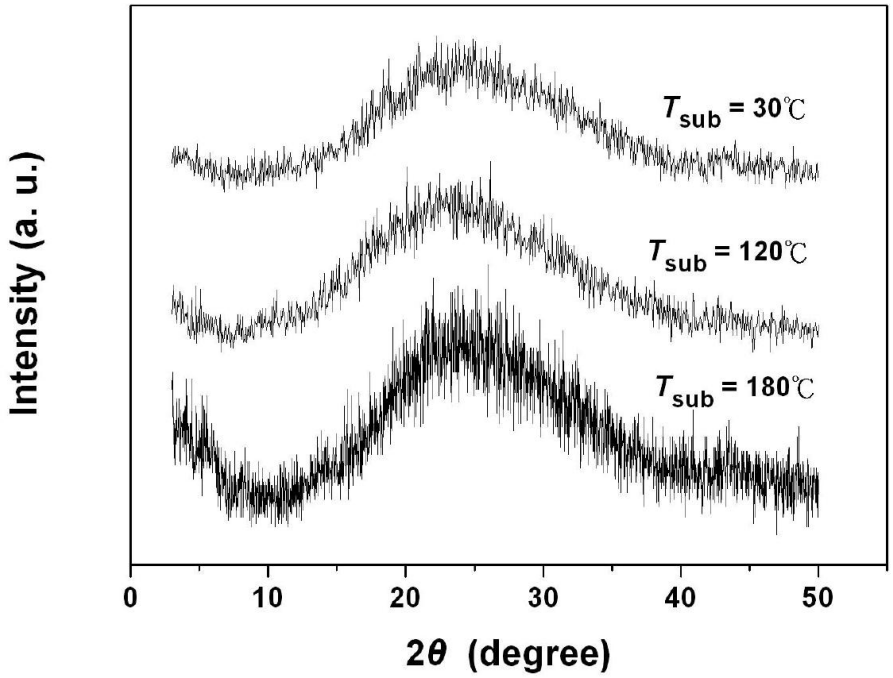

Fig. 3 XRD patterns for Alq3 layers deposited at different T_{sub}.

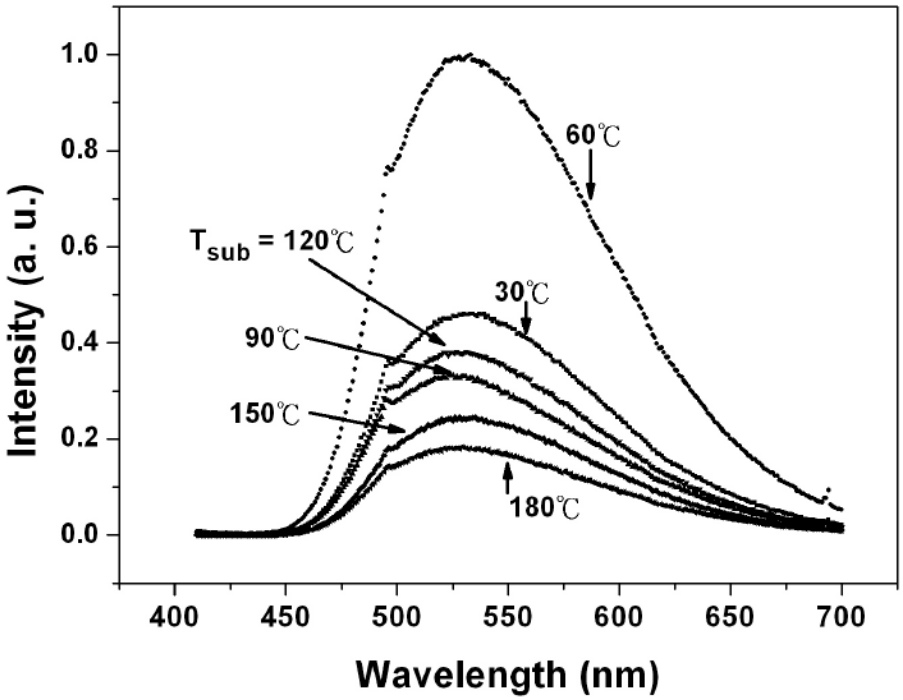

Fig. 4 Room temperature PL studies for Alq3 layers deposited at different T_{sub}.

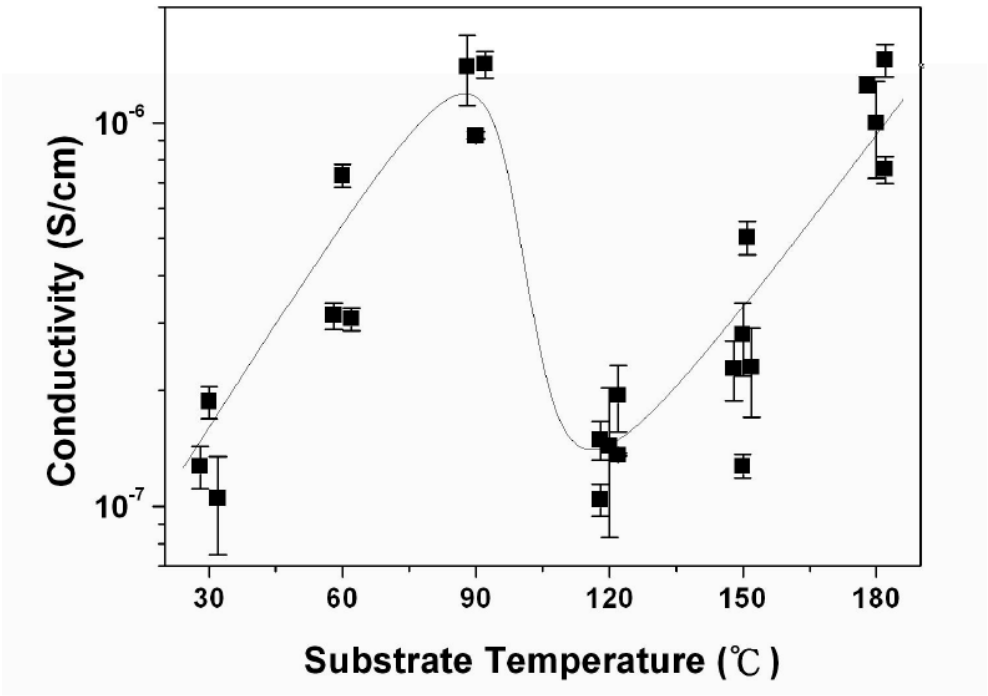

Fig. 5 Values of $\sigma(T = 300\text{K})$ for Alq3 layers with respect to different T_{sub}.

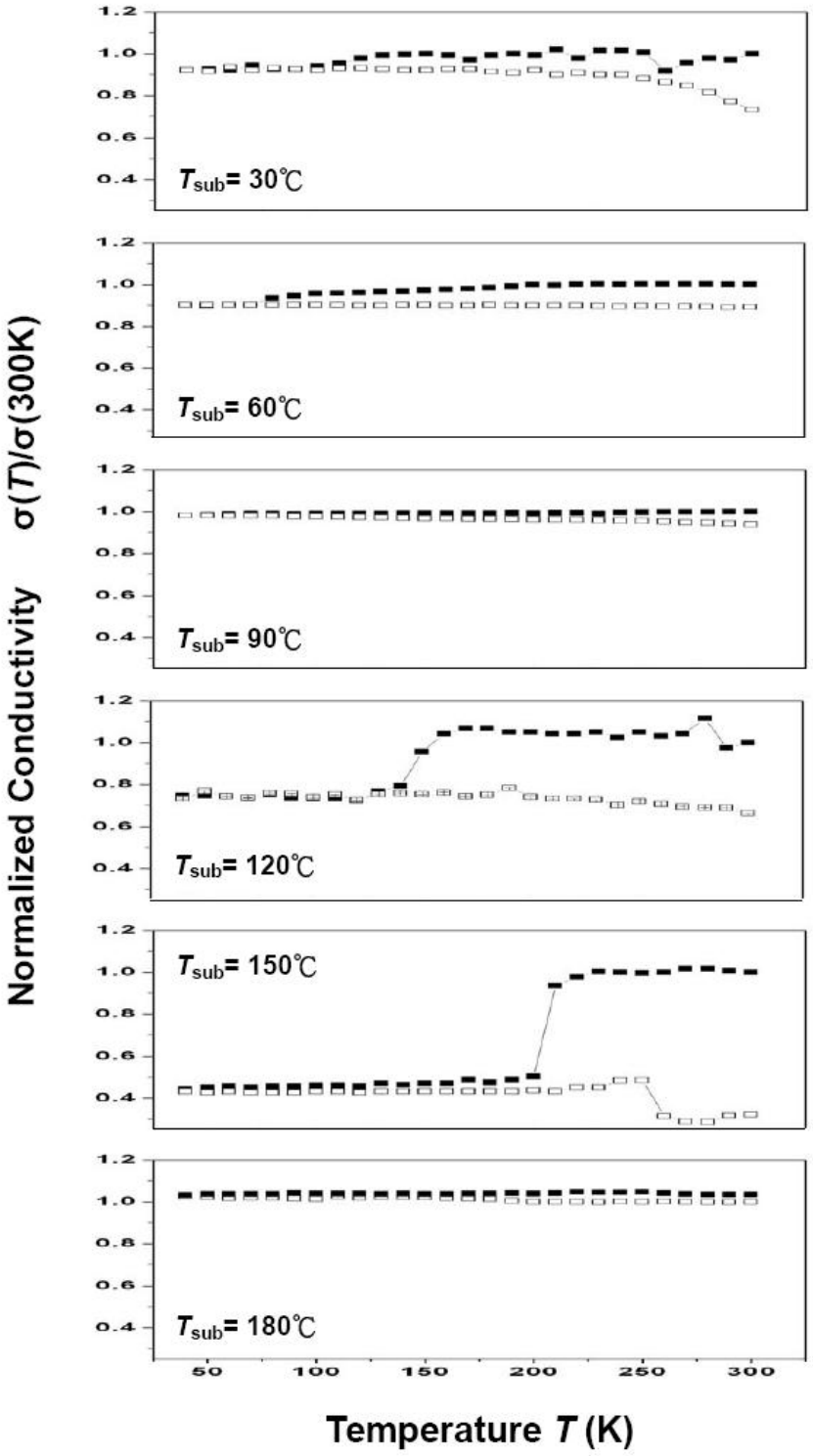

Fig. 6 Temperature dependence of normalized conductivity $\sigma(T)/\sigma(T = 300\text{K})$ for Alq3 layers deposited at different T_{sub}. Solid symbols indicate for decreasing T-scan and open symbols for increasing T-scan.